PHYSICAL REVIEW B VOLUME 43, NUMBER 8 15 MARCH 1991-I

Interface effects of hydrogen uptake in Mo/V single-crystal superlattices

B. Hjörvarsson, J. Rydén, and E. Karlsson
Department of Physics, Uppsala University, P. O. Box 530, S-751 21 Uppsala, Sweden

J. Birch and J.-E. Sundgren
Department of Physics, Linköping University, S-581 83 Linköping, Sweden

(Received 25 April 1990)

Results from measurements of the hydrogen uptake in Mo/V single-crystal superlattices with modulation wavelengths (Λ) from 0.3 to 17.7 nm are presented. These studies were performed by hydrogen profiling, using the $^1H(^{15}N,\alpha\gamma)^{12}C$ reaction, and x-ray diffraction. The average hydrogen to metal ratio was found to decrease for decreasing Λ. For $\Lambda \geq 13$ nm, large structural changes are observed, while for $\Lambda \leq 5.5$ nm no structural changes were observed upon hydrogenation. A model describing the modulated-wavelength dependence of the hydrogen uptake is proposed.

INTRODUCTION

The interest in layered metallic structures (superlattices) has increased dramatically during the past decade. A number of laboratories have facilities to produce and study the properties of metallic superlattices, sometimes with technical applications in mind. The properties of each layer differ in several respects from the corresponding bulk material, and the macroscopically measured properties are not the same as those of random alloys of the same nominal composition. Some examples of layer-specific properties are magnetism in thin Co layers between Pd layers,[1] the giant magnetoresistivity observed for Fe/Cr superlattices,[2] the supermodulus effect observed in several superlattices with fcc structure, e.g., TiN/VN,[3] and the increased solubility of hydrogen in Nb/Ta superlattices.[4] The possibility of performing "layer-by-layer engineering" to achieve specific properties is attractive. The basic description of electron structure, etc., for these materials, is, however, still quite rudimentary, and more experimental as well as theoretical work is required.

One interesting aspect of the metallic superlattices is their ability to absorb gases, in particular hydrogen. It is known from studies on bulk materials that this capacity is strongly tied to the electron structure of the host, and certain hydride forming metals have a large negative heat of solution for hydrogen. The present experiment aims at an understanding of the change in the binding energy of hydrogen in superlattices of Mo/V when the thicknesses of the individual layers are decreased to a few monolayers of each of the constituents. The heat of solution for hydrogen in vanadium is -0.30 eV/H, whereas for molybdenum it is positive with a value of 0.41 eV/H.[5] There might be several reasons for a change in the hydrogen solubility of superlattices compared to the bulk solubilities of the constituents. Band-bending effects near the interfaces, change of crystal parameters due to strain in the epitaxially grown layers (which may even prevent the α- to β-phase transition in V for higher H concentrations), and specific absorption of H in the interfaces are such examples. In our experiments crystallographic changes have been measured by x-ray diffraction (XRD), and the hydrogen concentrations are determined by hydrogen profiling using the ^{15}N nuclear reaction.

SAMPLE PREPARATION

The Mo/V superlattices were grown epitaxially on polished (100)-oriented MgO substrates in a diffusion-pumped sputtering system, having an ultimate pressure of 8×10^{-8} mbar (8×10^{-6} Pa). The system was equipped with two dc planar magnetron cathodes each with an independently controlled shutter. The accuracy of the deposition time was 0.1 s and in order to reduce intermixing at the interfaces both shutters were kept closed for 0.25 s between the deposition of each layer. The MgO substrates were annealed *in situ* at 800 °C at a pressure of less than 2.7×10^{-6} mbar (2.7×10^{-4} Pa) for 1 h prior to growth, in order to produce clean and well-ordered surfaces. The deposition of the superlattices was initiated after lowering the substrate temperature to 700 °C and sputter cleaning the molybdenum and vanadium targets with argon (99.9997% purity). The deposition rates were determined from microstylus measurements and by XRD measurements from periodic superlattices with asymmetric periods.[6] Furthermore, the modulation wavelengths and elemental composition were confirmed by XRD and Rutherford backscattering analysis. Typically the rates were found to be in the range of 0.20–0.37 nm/s for Mo and 0.16–0.27 nm/s for V.

The hydrogen uptake of superlattices is strongly affected by the surface conditions and the temperature during hydrogenation. Therefore samples were prepared in such a way that each was built up of five or six consecutive superlattices with different modulation wavelengths (Λ). *Thus each of these multilayered superlattices (MLSL's) effectively contained several samples.* This preparation technique was used to ensure thermodynamic equilibrium within the series of different Λ. Those with

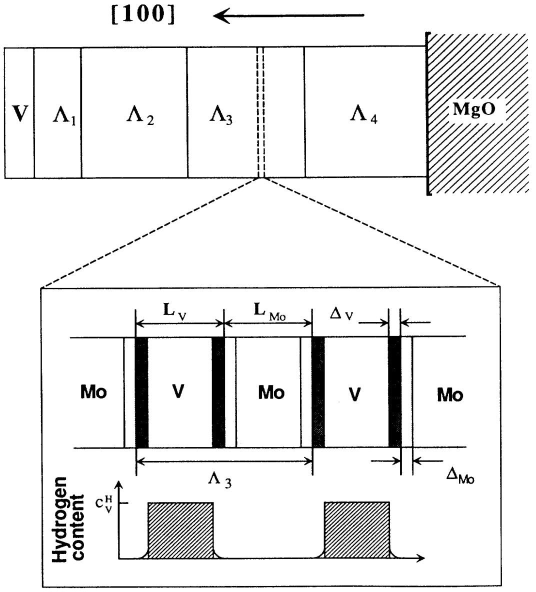

FIG. 1. Illustration of a multilayered superlattice which consists of four different superlattices with different Λ. The hydrogen concentration is high in the vanadium layers but negligible in the molybdenum ones. The hydrogen content at the vanadium interfaces is described by the function $f(L_V, L_{Mo})$. The orientation of the crystal is indicated in the figure.

the smallest Λ were placed nearest to the surface where the depth resolution of the nitrogen-15 method is at its best. The surfaces were covered by 10-nm V layers in order to obtain identical surface conditions for all the samples. The essence of this is illustrated in Fig. 1. In sample No. 1, the ratio between the individual layer thicknesses L_{Mo}/L_V was kept constant at 0.73 throughout the MLSL and Λ was increased with increasing depth. In contrast, the thickness of the molybdenum layers was kept constant (1.8 nm) in sample No. 2 while Λ and consequently the vanadium thickness were increased with increasing depth. In sample No. 3 the vanadium layer thickness remained the same (1.5 nm), while the molybdenum thickness, and hence Λ, varied. The modulation wavelength in the MLSL series was always lower than the critical layer thickness (6 nm) at which the layers start to grow three dimensionally.[7] This is to ensure small variation in the modulation wavelengths.

The hydrogenation was performed in a diffusion pumped cell with a base pressure of 6.6×10^{-7} mbar (6.6×10^{-5} Pa). Prior to hydrogenation all samples were annealed at 400 °C for between 4 and 12 h, thereafter they were hydrogenated at 125 °C or 225 °C for 30 or 240 min and cooled down to room temperature in H_2 atmosphere. All hydrogenations were performed at a pressure of 1.0-bar H_2 (99.9997% purity).

EXPERIMENTAL DETAILS

In order to investigate the structural changes of the superlattices containing only one modulation sequence, XRD spectra were recorded from the superlattices (Λ = 17.7, 13.3, 5.5, 3.5, and 2.0 nm) before and after hydrogenation. All the XRD spectra were recorded by powder diffractometry with an accuracy of 0.01° in 2θ. Unmonochromatized Cu radiation containing both characteristic $K\alpha_1$ and $K\alpha_2$ radiation was used.

The profiling measurements were made at the Tandem Accelerator Laboratory in Uppsala, Sweden. The analyzing chamber is pumped with a cryopump giving a working pressure in the lower 10^{-9}-mbar region (10^{-7} Pa). The hydrogen concentration was determined using the nuclear resonance reaction ${}^{1}\mathrm{H}({}^{15}\mathrm{N},\alpha\gamma){}^{12}\mathrm{C}$ with resonance energy $E_{res} = 6.385$ MeV. The samples were bombarded with ^{15}N ions having an energy higher than or equal to the resonance energy ($E \geq E_{res}$). While penetrating the sample the ions lose energy. When the ion energy is equal to E_{res} the cross section for the reaction increases and a number of γ quanta, with an energy of 4.43 MeV, proportional to the hydrogen concentration at that depth are produced. Knowing the specific energy loss (dE/dx) of the ^{15}N ions in the sample material, the depth (x) at which the reaction occurs can be estimated from the following formula:

$$x = \frac{E - E_{res}}{\left.\dfrac{dE}{dx}\right|_{E_{res}}} . \tag{1}$$

A NaI detector (125.6×15.24 cm^3) placed at a distance of 5 cm from the sample, at an angle of 0° with respect to the incident beam, was used for detection of the γ quanta. The beam current is integrated in the chamber, which is insulated from the beam line. This gives the total number of ions impinging on the sample. The diameter of the beam at the surface of the sample was 2 mm. Due to good thermal contact with the sample holder, which is cooled by liquid nitrogen, no significant macroscopic increase of the sample temperature is believed to occur during analysis. This is verified by the reproducibility of the results. The energy spread of the beam (Γ_{tot}) is dominated, close to the surface, by the vibrational motion of the hydrogen through the Doppler term in the reaction kinematics. As the depth increases, the energy straggling becomes the major contribution to the energy spread.[8] All samples were tilted during profiling.

RESULTS AND DISCUSSION

Both high- and low-angle XRD spectra were recorded from the five superlattices with a modulation wavelength (Λ) falling in the range 2.0–17.7 nm before and after hydrogen loading. No changes were observed upon hydrogenation for Λ ≤ 5.5 nm, whereas for Λ ≥ 13.3 nm large structural changes were observed. This is illustrated in Fig. 2. For the sample with Λ = 5.5 nm, Bragg reflection, as well as the intensities of the satellites, remains the same. Large structural changes are observed for the sample with Λ = 13.3 nm, which is associated with an α- to β-phase transformation in the hydrogen-containing vanadium layer.

From profiling measurements on several samples, hy-

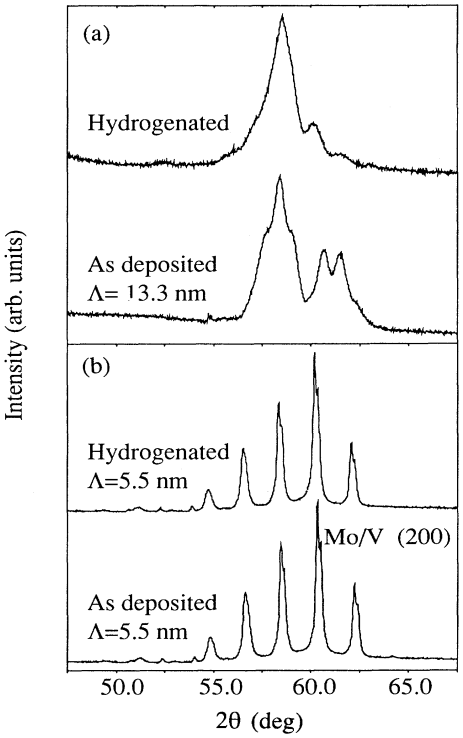

FIG. 2. High-angle XRD spectra from samples with Λ equal to 5.5 and 13.3 nm, before and after hydrogenation. The details are given in the text.

drogenated for 30 min at moderate temperatures (as low as 125 °C), no concentration gradients were observed, even for thicknesses up to 8.8 nm of Mo. This verifies that thermodynamic equilibrium was established throughout the samples, and also that the transport properties of hydrogen in Mo films might be underestimated.

The modulation wavelengths of the MLSL's varied from 0.3 to 6.7 nm. By transforming the thicknesses of the layers into the energy loss of the ions, a simple and a straightforward formalism is obtained. The equation for the energy lost by the ions (ΔE_j) penetrating a layer j of thickness L_j, having specific energy loss $(dE/dx)|_j^E$, reads

$$\Delta E_j = \left.\frac{dE}{dx}\right|_j^{E} L_j \; . \tag{2}$$

For long wavelengths $(\Delta E_j + \Delta E_{j+1} \gg \Gamma_{\text{tot}})$ it is possible to determine the concentration in the individual layers. In Fig. 3 the hydrogen profile of a hydrogenated Mo/V $(\Lambda = 13.3$ nm) single superlattice is illustrated together with a simulation of the normalized yield (for details of the simulation see Ref. 9). The hydrogen concentration in the molybdenum layers was below the detection limit. In the vanadium layers the *average* H/V atomic ratio was found to be 0.33(2) for all vanadium layers, except those closest to the surface. The hydrogen concentration is below that expected for pure vanadium,[9] which will be shown to be related to interface effects.

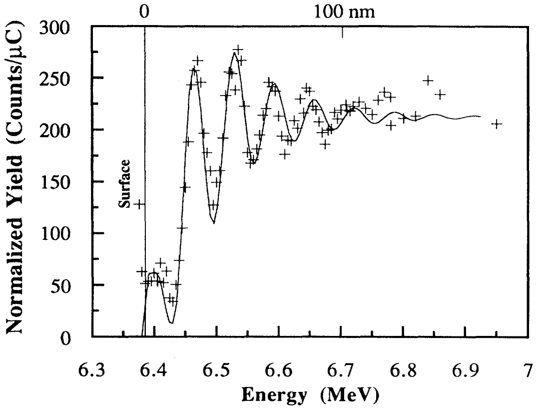

FIG. 3. Normalized yield vs energy for a Mo/V superlattice with $\Lambda = 13$ nm, hydrogenated at 225 °C and 1 bar for 30 min. The solid line is a simulation of the profile assuming that all hydrogen is in the vanadium layer. The average N_y is 212 counts/μC.

For short wavelengths or at large depths $(\Delta E_j + \Delta E_{j+1} \ll \Gamma_{\text{tot}})$, the nitrogen-15 method gives the average hydrogen concentration in the molybdenum and vanadium layers. This is clearly seen, for energies higher than 6.9 MeV, in Fig. 3 where the energy resolution is lost due to the energy straggling. When $\Delta E_j + \Delta E_{j+1} \ll \Gamma_{\text{tot}}$, the yield (Y_j) from a layer j in the sample is given by

$$Y_j = K \frac{\langle c_j^H \rangle Q_j}{\left.\dfrac{dE}{dx}\right|_j^{E_r}} \; , \tag{3}$$

where K is a calibration constant obtained from a calibration sample with known hydrogen concentration,[11] which includes the resonance cross section, the detector efficiency, the solid angle, and the angular distribution of the γ radiation. The measured yield consists of two contributions; the yield from the nuclear reaction and a background contribution which is subtracted. The measured average hydrogen concentration is denoted $\langle c_j^H \rangle$, Q_j is the total number of ions having the resonant energy (E_r) in the layer j, and $(dE/dx)|_j^{E_r}$ is the specific energy loss at the resonance energy in that layer. The total yield from the sample is a summation of the yield from the individual layers and for the actual superlattices it can be factorized into two components, one corresponding to the vanadium and the other to the molybdenum layers. Furthermore, the number of particles in a layer, at the resonance energy, is directly proportional to the energy lost by the ions in that layer. Taking this into account and using the normalization condition $(Q_{\text{tot}} = Q_{\text{V}} + Q_{\text{Mo}})$, where Q_{tot} is the total number of ions hitting the sample, and also assuming that the hydrogen content of the Mo layer is negligible, Eq. (3) gives the following expression for the normalized yield from a superlattice:

$$N_y=\frac{Y}{Q_{\mathrm{tot}}}=\frac{K\langle c_{\mathrm{V}}^{\mathrm{H}}\rangle}{\left.\frac{dE}{dx}\right|_{\mathrm{V}}^{E_r}\left[1+\frac{L_{\mathrm{Mo}}\left.\frac{dE}{dx}\right|_{\mathrm{Mo}}^{E_r}}{L_{\mathrm{V}}\left.\frac{dE}{dx}\right|_{\mathrm{V}}^{E_r}}\right]}\ . \tag{4}$$

Here the individual layer thicknesses of molybdenum and vanadium are denoted L_{Mo} and L_{V}. The normalized yield is displayed in Fig. 4 for different energies for sample No. 1. The trend is unambiguous: increasing yield with increasing Λ.

By assuming that an interface layer with the thickness Δ_{V} in vanadium is almost hydrogen free, the following expression is obtained for the average hydrogen concentration in the vanadium layer:

$$\langle c_{\mathrm{V}}^{\mathrm{H}}\rangle=\eta c_{\mathrm{V}}^{\mathrm{H}}\left[1-\frac{2\,\Delta_{\mathrm{V}}}{L_{\mathrm{V}}}\right]+f(L_{\mathrm{V}},L_{\mathrm{Mo}})\ . \tag{5}$$

Here the actual concentration in the high-concentration region, as illustrated in Fig. 1, is denoted by $c_{\mathrm{V}}^{\mathrm{H}}$, the average concentration in the whole V layer by $\langle c_{\mathrm{V}}^{\mathrm{H}}\rangle$, and the function η is zero for $L_{\mathrm{V}}<2\,\Delta_{\mathrm{V}}$ and unity otherwise. The function $f(L_{\mathrm{V}},L_{\mathrm{Mo}})$ is a correction for the hydrogen content of the interface layers, and dominates the average concentration as L_{V} is decreased to $2\,\Delta_{\mathrm{V}}$ and below. By combining Eqs. (4) and (5), an expression relating the normalized yield to the thickness of the individual layers is obtained:

$$N_y=\frac{\eta K c_{\mathrm{V}}^{\mathrm{H}}\left[1-\frac{2\,\Delta_{\mathrm{V}}}{L_{\mathrm{V}}}\right]}{\left.\frac{dE}{dx}\right|_{\mathrm{V}}^{E_r}\left[1+\frac{L_{\mathrm{Mo}}\left.\frac{dE}{dx}\right|_{\mathrm{Mo}}^{E}}{L_{\mathrm{V}}\left.\frac{dE}{dx}\right|_{\mathrm{V}}^{E_r}}\right]}+F(L_{\mathrm{V}},L_{\mathrm{Mo}})\ . \tag{6}$$

The function $F(L_{\mathrm{V}},L_{\mathrm{Mo}})$ scales as $\Delta_{\mathrm{V}}/\Lambda$ for $L_{\mathrm{V}}>2\,\Delta_{\mathrm{V}}$ and $L_{\mathrm{Mo}}>2\Delta_{\mathrm{Mo}}$, and when $L_{\mathrm{Mo}}\rightarrow 0$ the hydrogen content of the interface layer approaches that of vanadium. Equation (6) can be simplified to emphasize the thickness dependence for large Λ ($L_{\mathrm{V}}\gg 2\,\Delta_{\mathrm{V}}$) as the contribution from the interface layers becomes small and can be neglected, thus $F(L_{\mathrm{V}},L_{\mathrm{Mo}})\rightarrow 0$:

$$N_y=\frac{D\left[1-\frac{2\,\Delta_{\mathrm{V}}}{L_{\mathrm{V}}}\right]}{\left[1+1.09\frac{L_{\mathrm{Mo}}}{L_{\mathrm{V}}}\right]}\ . \tag{7}$$

The values for $(dE/dx)|_{\mathrm{Mo}}^{E_r}$ and $(dE/dx)|_{\mathrm{V}}^{E_r}$ were obtained from a Fortran code based on the stopping power compilation of Ziegler *et al.*[12] and all parameters and constants that do not depend explicitly on Λ have been combined in a single constant D. For sample No. 1 with the constant $L_{\mathrm{Mo}}/L_{\mathrm{V}}$ ratio, Eq. (7) becomes extremely simple; the normalized yield is expected to scale linearly with the inverse thickness of the vanadium layer.

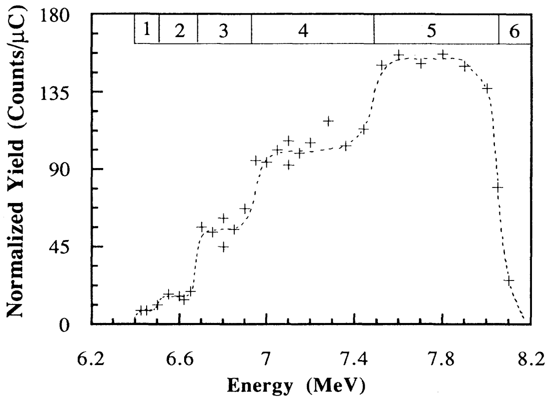

FIG. 4. Normalized yield vs energy for a multilayered single-crystal superlattice with $L_{\mathrm{Mo}}/L_{\mathrm{V}}$ equal to 0.73, hydrogenated at 225 °C and 1 bar for 4 h. The thicknesses are as follows from the surface into the bulk [layer number, Λ (nm); total thickness of layer (nm)]: (1, 0.34, 73)-(2, 1.0, 142)-(3, 2.3, 213)-(4, 3.3, 443)-(5, 6.7, 533).

The average normalized yield is plotted against the inverse layer thickness of vanadium ($1/L_{\mathrm{V}}$) in Fig. 5. The interface layer (Δ_{V}) is found to be 0.49 nm by fitting Eq. (7) to the normalized yield for large Λ. It was not possible to distinguish between the contribution from the mixing of the layers and effects arising solely from the charge transfer from the molybdenum to the vanadium layers. The mixing of the interfaces was previously found to be plus or minus one $\langle 100\rangle$ lattice plane, which corresponds to ±0.15 nm.[7]

The results from hydrogen profiling measurements of samples No. 2 and No. 3, illustrated in Fig. 6, supports the simple model described above. The solid line is a prediction of the normalized yield, neglecting the correction term, obtained by substituting the best-fit data from analysis of sample No. 1 in Eq. (6). For sample No. 2 the

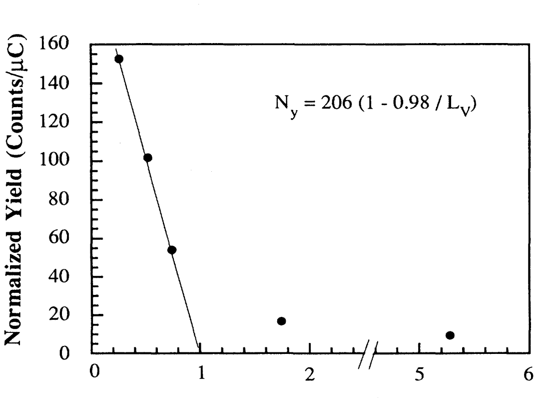

FIG. 5. Normalized yield as a function of the inverse thickness L_{V}. The H/V atomic ratios are 0.34(2) in the high-concentration region ($c_{\mathrm{V}}^{\mathrm{H}}$).

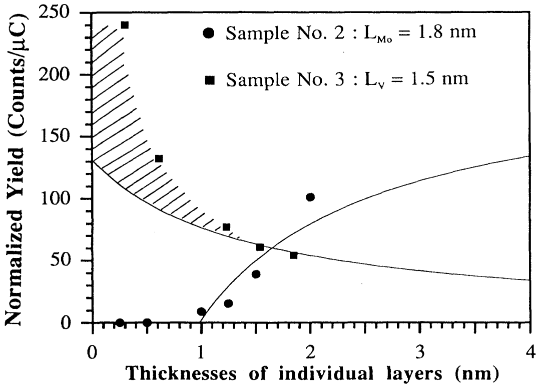

FIG. 6. Normalized yield for samples No. 2 and No. 3. The solid line is obtained by substituting parameters, from the best fit to data obtained from the analysis of sample No. 1, in Eq. (7). In sample No. 3 the "correction term" becomes large for small Λ, and hence cannot be neglected. The contribution associated with the correction is shaded in the figure. By assuming that the heat of solution scales linearly with the electron density, as described by effective medium theory, the correction term will depend exponentially on the modulation wavelength when $L_{\mathrm{Mo}} \rightarrow 0$.

correction term was found to be small, as the superlattice is hydrogen free when the thin vanadium layer has coupled to the molybdenum layer and the hydrogen uptake is presumably governed by the charge transfer at the interfaces. In sample No. 3 the hydrogen content increased more rapidly than the predicted asymptotic behavior for small Λ. This is a consequence of the gradual decrease in the electron density at the interface layers with decreasing L_{Mo}.

The decrease (increase) of hydrogen uptake with increasing (decreasing) electron density can be explained in terms of effective-medium theory,[13] assuming a charge transfer at the interfaces. In this instance we have not considered the actual form of the screening function. Another possible explanation for the decreased hydrogen uptake is the strain induced by the lattice mismatch. This causes the lattice parameter, in the plane parallel to the sample surface, to increase in vanadium and decrease in the molybdenum layers, while the contrary is valid for the lattice parameter perpendicular to the sample surface. For very short modulation wavelengths (up to three to four monolayers) the interfaces are coherent, and therefore the molybdenum and the vanadium layers are maximally strained. With increasing modulation wavelength, an increasing number of misfit dislocations are formed close to the interfaces. Consequently, the strain decreases with increasing modulation wavelength. It is not possible to deduce the strain in the individual layers by θ-2θ XRD, since an average lattice parameter is measured. In a biaxial state of tensile strain, as in the vanadium layers in the Mo/V superlattices, the volume increases with increasing strain. Hence the electron density is expected to decrease with decreasing Λ. This implies, according to effective-medium theory, that hydrogen content increases with decreasing Λ, which is in contradiction to our results. Therefore we expect the charge-transfer mechanism to be the dominating contribution to the decreased solubility of hydrogen in the vicinity of the interfaces. However, the hydrogen uptake is also suppressed by the elastically mediated hydrogen-hydrogen interaction in the strained lattice. This is seen by the suppressed uptake of hydrogen in the high-concentration region of vanadium. In a recent study[14] Miceli and Zabel reported an enhanced hydrogen uptake of Nb/Ta superlattices, a result which is believed to be solely strain induced. As both niobium and tantalum have similar electron densities, at the hydrogen site, no interface effects similar to those observed here would be expected.

The vanadium layer, for large Λ, consists of two distinct regions. The center of each layer contains large amounts of hydrogen while at the interfaces the concentration is low and thus the assumption made here is legitimate as a first approximation. The mean electron density $\bar{n}_0$ of the host is assumed to describe the electron density at the hydrogen site and is defined as in Ref. 13. To calculate the population of sites in the vicinity of the interface demands a knowledge of the form of the screening, the degree of hybridization, and the cohesive energy of the interface, which is beyond the scope of this paper.

The hydrogen binding energy in the host material can be written in the following way:[13]

$$\Delta E = \Delta E_{\mathrm{eff}}^{\mathrm{hom}}(\bar{n}_0) + \Delta E^{\mathrm{hyb}} \ . \tag{8}$$

The change in the heat of solution for hydrogen in vanadium with electron density is found by differentiating Eq. (8) with respect to $\bar{n}_0$. This approach is adequate as it is only the change in the binding energy in the host material which is of concern. Even though the contribution of the hybridization to the total energy (ΔE^{hyb}) is large, it is fairly constant for the 3-*d* elements in the vicinity of vanadium (see Ref. 13, p. 2883, Fig. 5) and therefore the derivative ($\delta \Delta E^{\mathrm{hyb}} / \delta \bar{n}_0$) is assumed to be zero. The change in energy can then be expressed in the following parametrized way using the analytic expression of Nörskov (see Ref. 13, p. 2882):

$$\delta \Delta E \approx \delta \Delta E_{\mathrm{eff}}^{\mathrm{hom}}(\bar{n}_0) = (796 \bar{n}_0 + 20.8) \delta \bar{n}_0 \ (\mathrm{eV}) \ . \tag{9}$$

To clarify this approach take sample No. 2 as an example where the thickness of the vanadium layer is decreased while the molybdenum layer is kept constant (1.8 nm). As L_V decreases, the average electron density increases and at a certain thickness becomes so high that the heat of solution in the layer becomes positive (it contains no hydrogen). The limit for this increase in the electron density is found by substituting the value of the heat of solution and $\bar{n}_0$ [-0.30 eV from Ref. 3 and $0.028 + \frac{1}{2} \delta \bar{n}_0 (a_0^{-3})$ from Ref. 13] in expression (9). An increase of at least 23% in the electron density is obtained neglecting the structural distortion of the vanadium layers due to lattice mismatch. It should be pointed out that the lattice distortion for bcc metals is much more important than in close-packed metals[15] for the heat of solution; hence careful calculations are needed for the interpretation of the change in energy upon lattice expansion (contraction).

CONCLUSIONS

The hydrogen uptake of Mo/V superlattices is evidently strongly dependent upon the modulation wavelengths, as unambiguously illustrated in the present work. This dependence is related to the charge transfer at the interfaces. The form of the electron density variation is still an open question, but in the model presented here this is solved by introducing a perturbation term which is shown to be small for large Λ, and vanishes when $L_V \rightarrow 0$. When $L_{Mo} \rightarrow 0$, the amplitude of the perturbation increases and by assuming that the heat of solution scales linearly with the electron density, the correction term will depend exponentially on the modulation wavelength when $L_{Mo} \rightarrow 0$. The effective screening length (Δ_V) was extracted from the variation of the hydrogen concentration for large Λ. The hydrogen "free" layers (Δ_V) were found to be 0.49 nm, which was then used for the simulations in Fig. 6. Presumably the electron-density variation is not as localized as assumed in the model; despite that, the model describes the asymptotic behavior of the hydrogen uptake well. This indicates that the charge-transfer mechanism is the dominating contribution to the decreased solubility in the vicinity of the interfaces. On the other hand, the decreased solubility of the high-concentration region of hydrogen in the vanadium layer can be related to the elastically mediated hydrogen-hydrogen interaction in the strained lattice. The negligible structural changes of superlattices with modulation wavelengths smaller than 5.5 nm are related to a suppression of the α- to β-phase transformation, hence the high-concentration α' phase is favorable for small wavelengths.

---

[1] M. Stampanoni *et al.*, J. Appl. Phys. **64**, 5321 (1988).

[2] M. N. Baibich *et al.*, Phys. Rev. Lett. **61**, 2472 (1988).

[3] U. Helmersson *et al.*, J. Appl. Phys. **62**, 481 (1987).

[4] P. F. Miceli, H. Zabel, and J. E. Cunningham, Phys. Rev. Lett. **54**, 917 (1985).

[5] R. Griessen, Phys. Rev. B **38**, 3690 (1988).

[6] J. Birch *et al.*, Phys. Rev. B **42**, 10 398 (1990).

[7] J. Birch *et al.*, Vacuum **41**, 1231 (1990).

[8] B. Hjörvarsson and J. Rydén, Nucl. Instrum. Methods B **45**, 36 (1990).

[9] J. Rydén and B. Hjörvarsson (unpublished).

[10] D. Richter, S. Mahlig-Ennaoui, and R. Hempelmann (unpublished).

[11] B. Hjörvarsson, J. Rydén, T. Ericsson, and E. Karlsson, Nucl. Instrum. Methods B **42**, 257 (1989).

[12] J. F. Ziegler, J. P. Biersack, and U. Littmark, *The Stopping and Ranges of Ions in Matter* (Pergamon, New York, 1985), Vol. 1.

[13] J. K. Nörskov, Phys. Rev. B **26**, 2875 (1982).

[14] P. F. Miceli and H. Zabel, Z. Phys. B **74**, 457 (1989).

[15] P. Nordlander, J. K. Nörskov, and F. Besenbacher, J. Phys. F **16**, 1161 (1986).